INTERNATIONAL SOCIETY FOR
SOIL MECHANICS AND
GEOTECHNICAL ENGINEERING

This paper was downloaded from the Online Library of the International Society for Soil Mechanics and Geotechnical Engineering (ISSMGE). The library is available here:

https://www.issmge.org/publications/online-library

This is an open-access database that archives thousands of papers published under the Auspices of the ISSMGE and maintained by the Innovation and Development Committee of ISSMGE.

The paper was published in the proceedings of the 7th International Conference on Earthquake Geotechnical Engineering and was edited by Francesco Silvestri, Nicola Moraci and Susanna Antonielli. The conference was held in Rome, Italy, 17 – 20 June 2019.

Earthquake Geotechnical Engineering for Protection and Development of Environment and Constructions – Silvestri & Moraci (Eds)
© 2019 Associazione Geotecnica Italiana, Rome, Italy, *ISBN 978-0-367-14328-2*

Effects of the Central Italy 2016 seismic sequence on slope stability: Preliminary analysis of some major rock slides

P. Tommasi & A. Di Giulio
CNR – Istituto di Geologia Ambientale e Geoingegneria, Rome, Italy

A. Santo, G. Forte & M. De Falco
Università di Napoli Federico II – Dipartimento di Ingegneria Civile, Edile e Ambientale, Naples, Italy

L. Verrucci, G. Lanzo & T. Rotonda
Sapienza Università di Roma– Dipartimento di Ingegneria Strutturale e Geotecnica, Rome, Italy

K.W. Franke
Department of Civil and Environmental Engineering - Brigham Young University, Provo, UT, USA

ABSTRACT: The August and October 2016 earthquakes caused several instability phenomena on rock slopes over a large area of the Apennine mountain chain. Major rock slides and rock falls were caused by the October earthquakes, which involved the northern part of the damaged area and surprisingly triggered relevant rock falls in the southernmost part. The distance from inhabited zones and roadways limited the consequences of larger failures with respect to their potential damage. After an overview of the rock instability phenomena, the geological setting of the area and the main features of 2016 earthquakes, selected major rock slides were examined in more detail. In situ and laboratory investigations are described, including UAV models of the slope morphology. Landslide geometry, rock mass structure and instability mechanisms are discussed, stressing critical aspects of their reconstruction. Finally, an attempt is made to link failure mechanisms to geological, structural and joint surface conditions and to features of local seismic motion, in the perspective of better appraising the seismic hazard in the region.

1 INTRODUCTION

The 2016 Central Italy seismic sequence was characterized by three major shocks (Figures 1 and 2): August 24th M_w6.0 (Accumoli, also named Amatrice earthquake), October 26th M_w5.9 (Ussita); October 30th M_w6.5 (Norcia). The latter is the strongest earthquake recorded after 1980 by the National Seismic Network (RAN- *Rete Accelerometrica Nazionale*).

Surface effects were recorded over an area of about 2000 km^2, which extends over four regions (Lazio, Abruzzo, Umbria and Marche). After the August 24th earthquake, more than 800 landslides, all few m^3 in volume, involving road cuts in rock and fill slopes were mapped by the Centre for Prediction, Prevention and Control of Geological Risks (Martino et al. 2017), the Geotechnical Extreme Events Reconnaissance Association (GEER, 2016) and the Institute for environmental protection and research (ISPRA, 2016). Except for Pescara del Tronto, landslides had limited or no interaction with the road network. Most of road cuts are excavated in the sandstone-mudstone flysch (*Laga Fm.*) that extensively outcrops in the area. Several rock falls also detached from the limestone formation outcropping in the northernmost part of the Amatrice earthquake damage area, upslope from the highways connecting Umbria and Marche regions (SS685 and SP477).

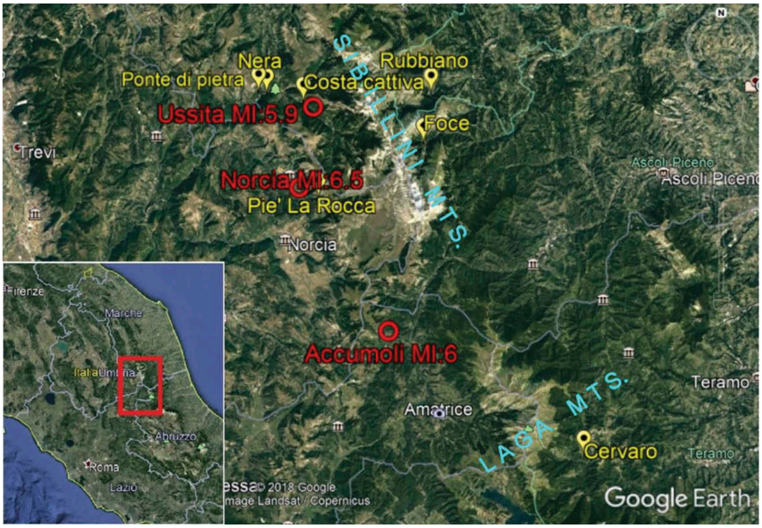

Figure 1. Epicentres of the three major 2016 earthquakes and location of the studied rock slides.

After the October earthquakes the most damaging landslide occurred in Visso, which caused the interruption of relevant roadways. These seismic events triggered many other landslides (Figure 2), mainly affecting the Sibillini Mts. National Park and Laga Mts. Few landslides involved rock slopes far to the south in Abruzzo Region. Martino et al. (2017) reported almost 250 and 400 instability phenomena after 26th and 30th October earthquakes respectively. Other landslides were reported by GEER (2017). The October 30th earthquake triggered also larger landslides up to 40,000 m^3 in volume, most of which were identified long time after the earthquake, when satellite/aerial images were allowable or UAV/field observation could

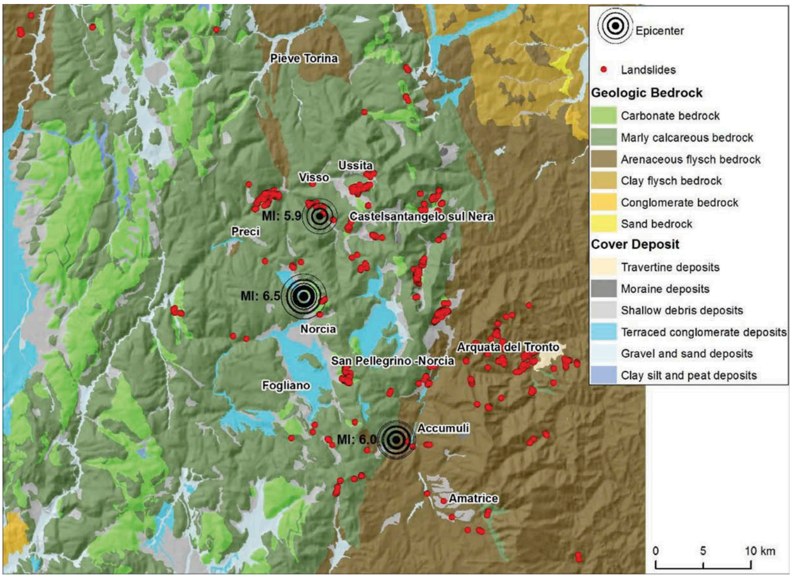

Figure 2. Geological sketch of the study area and distribution of the landslides triggered on natural slopes.

be conducted once safety conditions and road serviceability were re-established. The largest landslides involving rock slopes only occasionally caused damage to infrastructures, touristic trekking circuits and the environment.

2 GEOLOGICAL OUTLINES OF THE AREA

The area affected by the 2016 seismic sequence falls within the Umbria-Marche Apennines, an arcuate fold and-thrust belt that occupies the outer zones of the Central-Northern Apennines. The geological setting is characterized by several tectonic units (from Lias to Miocene), composed of massive and layered limestones (*Calcare Massiccio Fm.* and *Maiolica Fm.* respectively), marly limestones (*Scaglia Fm.*), marls and flysch deposits (e.g. *Laga Fm.*). The ridges primarily consist of Meso-Cenozoic carbonate host-rocks (Sibillini Mts.), locally covered by Miocenic marly limestones and sandstone/mudstone alternations. The arcuate shape is the result of a two-stage compressional history, which was active from the late Miocene to the beginning of the early Pliocene. During the first stage, a linear NW–SE to NNW–SSE striking fold belt developed in the sedimentary cover. During the second stage, shortening was prevailingly accomplished by thrusting on low-angle planes that propagated upward from the deep basement. After the main compressive phase, in the upper Pliocene the area was definitively uplifted and the compressive structures were dissected by normal faults during the Quaternary (Boncio and Lavecchia, 2000 and references therein).

The structural setting is controlled by the thrusting of the Meso-Cenozoic units on the arenaceous-pelitic sequences (*Laga Flysch Fm.).* The Quaternary normal faults led to the formation of intramountain basins (e.g. Colfiorito and Castelluccio plains) bounded by seismogenic faults. Alluvial and lacustrine deposits are found in the intramountain basins; they can reach a thickness of 100 m and are formed by more or less regular alternations of conglomerates, clays and sands and are dated to lower-middle Pleistocene. Finally, travertine deposits (middle Pleistocene up to now.) mainly formed by spring water whose chemical content is connected to the activity of deep faults and fractures can be found (Quattrocchi et al., 2000). In Figure 2 a simplified geo-lithological sketch of the main outcropping terrains is reported.

The geomorphologic setting is characterized by a general conformity between the structural-lithologic elements and the morphologies. High relief zones are represented by calcareous ridges highly and smooth areas correspond to the flysch deposits. Even the drainage network is influenced by the structural pattern and the main drainage lines are located along the trace of the main faults and fractures.

The present tectonic activity is testified by the recent seismic sequence (2016–2017) and several destructive historical earthquakes (1328, 1349, 1703, 1730, 1979, 1997), whose focal solutions are consistent with an extensive regime (Boschi et al., 1997 and references therein).

Landslides represent the main ground effects caused by the 2016-2017 seismic sequence, which triggered more than 1500 events (Figure 2), mostly rock falls. Field observations have shown that the landslides mainly affected the limestones and subordinately the sandstones of the *Laga* flysch. They occurred on high steep slopes, the edge of embankments of terraced deposits and road cuts.

3 INVESTIGATIONS

Structural data and information on the surface conditions of major discontinuities were obtained from processing of UAV imagery. In some cases, the results were verified on the basis of site measurements of the attitude of bedding and discontinuities taken within the landslide scar. In many cases, height and steepness of rock slopes, as well as the poor safety conditions induced by failures, inhibited direct access. All UAV surveys were performed by the Brigham Young University (BYU) during three campaigns in 2016 and 2018, except for the survey of Piè la Rocca rock slide, commissioned by Sapienza University in late 2018.

Data on small-scale strength of rock joints and on dynamic stiffness of the rock mass were taken from technical and scientific literature on the same rock formations. Only for the Nera rock slide mechanical properties of the rock material were determined on specimens cored from blocks retrieved from the landslide deposit.

In situ values of elastic wave velocity were obtained from literature data on the same lithotypes and scaled on the basis of rock mass fracturing and loosening.

3.1 *UAV surveys performed by BYU*

3.1.1 *Platforms*

One commercial off-the-shelf (COTS) UAV platform and one modified/customized COTS UAV platform were used in imaging landslides in the Central Italy earthquake reconnaissance. These platforms are shown in Figure 3. The majority of the landslide aerial imaging was performed with the DJI™ Phantom 4 quadrotor platform (Figure 3a). The Phantom 4 is equipped with a 4K video camera that has a 1/2.3" CMOS sensor, 94-degree field of view, 12.4 MP images, and a focal length of infinity. An Align™ TRex 800e helicopter UAV platform modified and customized for aerial photography (Figure 3b) was used to image the rock fall at SR-477 due to its capability to maintain stable flight in higher velocity winds. The TRex 800e has a 3-axis nose gimbal and uses a Nikon™ D750 DSLR camera with 24 MP image resolution, 35.9x24.0 CMOS image sensor, and 35 mm fixed focal length lens.

3.1.2 *Structure from motion photogrammetry software*

One of the most common forms of UAV-based remote sensing involves the use of lightweight optical sensors and a computer vision technique called Structure from Motion (SfM) (Marr and Nishihara 1978; Snavely et al. 2008). For this particular study, commercial SfM software programs ContextCapture by Bentley Systems, Inc.

Following tie point extraction using a scale invariant feature transform (SIFT) algorithm (Lowe 2004), camera internal parameters were used to develop a sparse point cloud on a local coordinate system. Surveyed ground control points (GCPs) were then used to anchor the sparse point cloud and reference it to global coordinates. Bundle block adjustment was then performed to adjust minimize location error in the sparse point cloud. Once adjusted, the sparse point cloud is populated with a dense point cloud using a variant of the semi global matching approach proposed by Hirschmüller (2005; 2008). Upon completion of the dense point cloud, various model products can then be developed including a three-dimensional meshed model, digital surface model (DSM), digital elevation model (DEM), and orthorectified aerial images.

3.2 *Geo-structural surveys*

For each rock slide, the 3D point cloud was analysed with the open source software Cloud Compare, which allows better visualization of geometry and morphology of natural surfaces

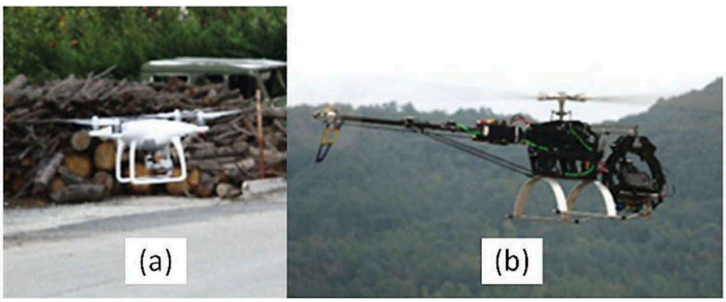

Figure 3. UAVs used for imaging of landslides during 2016 Central Italy reconnaissance

Table 1. Mean values of the physical and mechanical intact rock properties

	ρ_d (Mg/m^3)	ρ_s (Mg/m^3)	n (%)	V_P (km/s)	V_S (km/s)	UCS (MPa)	σ_t (MPa)
Ma	2.65	2.72	2.7	6.0	2.9	53	4.0
CM	2.68	2.75	2.5	6.1	3.2		4.5

by extracting linear and angular data. Orientation, medium- to large-scale roughness, persistence and extent of possible rock bridges were estimated.

At Nera and Pie' la Rocca rock slides, direct measurements of orientation and roughness were taken at spot with conventional techniques to confirm and calibrate calculations based on interpolation of point coordinates extracted from the digital models; extensive traditional surveys were not feasible.

3.3 *Mechanical properties of the rock material*

A limited number of laboratory tests were conducted, according to the ISRM standards, on specimens cored from limestone blocks retrieved at the foot of the Nera rock slide; rocks belong to the *Maiolica* (*Ma*) and *Calcare Massiccio (CM)* formations. Results are summarized in Table 1.

ρ_d: bulk dry density; ρ_s: density of the solid matrix; n: porosity; V_P, V_S: longitudinal and shear wave velocity; σ_t: indirect tensile strength; UCS: uniaxial compression strength

4 INVESTIGATED ROCK SLIDES

The study of the rock slides triggered by the 2016 earthquakes is in progress. Its aim is to acquire information on the dynamic behaviour of rock slopes involving geological units that outcrop in a wide area of Central Italy. Results of this study can be of general interest for this high-seismicity area and can help in developing a more accurate seismic hazard evaluation in this area and in a better understanding of instability mechanisms for design of stabilization measures.

The rock slides presented in this study are located near Visso and Norcia, as shown in Figure 1. Main features are summarized in Table 2.

Table 2. Main features of the investigated rock slides

Landslide	Epicentral distance (km)	Estimated volume (m^3×10^3)	Lithology
Nera (Sasso Pizzuto Mt.)	10.3*	32	Layered limestones (*Maiolica Fm.*)
Costa Cattiva (Nera River Valley)	8.7*	0.4	» »
Piè La Rocca	14.9°	15	Massive limestones (*Calcare Massicio Fm.*)
Ponte di Pietra (Nera gorge)	10.5*	7	» »
Foce	12.2*	30	» »
Rubbiano (Infernaccio gorge)	16.8*	15	Layered limestones (*Maiolica Fm.*)
Cervaro	40.5*	0.17	Sandstone/mudstone alternations (*Laga Fm.*)

* October 30th earthquake; °August 24th earthquake

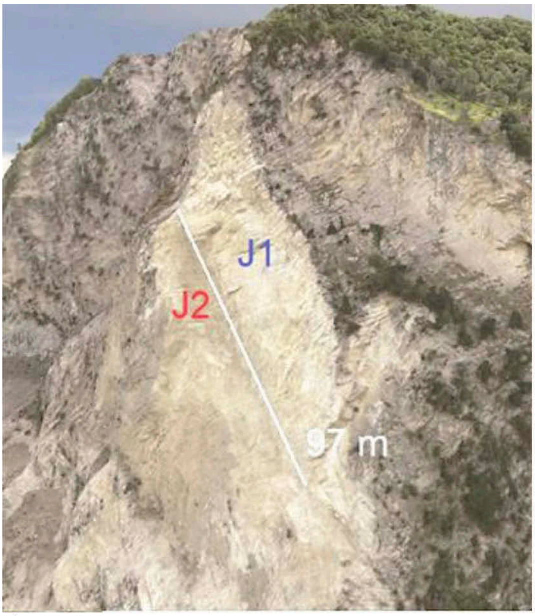

a)

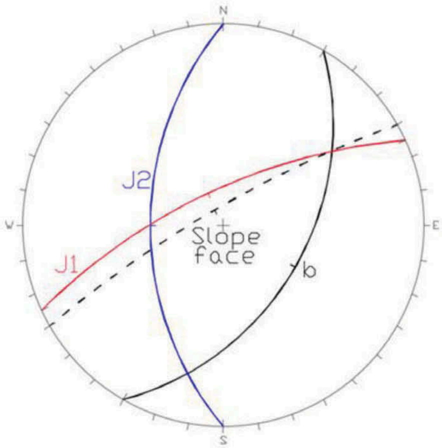

b)

Figure 4. Frontal view from the UAV survey of the Nera rock slide (a) and stereoplot (equal-area projection) of major discontinuities (b). In figure a) the two sliding surfaces are indicated; bedding planes, b in figure (b), dipping toward the rock mass are evident in the photograph a).

4.1 *Nera rock slide*

The Nera rock slide was investigated more extensively than the other failures occurred in this area because debris dammed the Nera River and blocked the road communication between the eastern and western part of Central Italy.

The landslide is a rock wedge-slide controlled by the intersection of very persistent fault planes and joints, which evolved into a rock avalanche. Wedge geometry was determined by calculating the orientations of the sliding surfaces and reconstructing the original cliff surface from the detailed 3D model obtained from the UAV surveys. During the demolition/recovery works on the cliff, joint orientations and joint surface conditions were verified with rope access surveys supported by experienced rock climbers.

Layers are less than 1m-thick and oriented 45°/120° (dip/dip direction), i.e. dipping against the slope, whilst the sliding surfaces J1 and J2 have an average orientation of 70°/335° and 50°/270° respectively (Figure 4). Figure 4 shows also the overall orientation of the rock cliff, here schematized as a single plane to better visualize the kinematics. According to a detailed analysis of the UAV models, the rock face is actually composed by two planes belonging to the same sets of the sliding surfaces, J2 and J1, which yield an estimated wedge volume of 32,000 m^3. The corresponding avalanche deposit assuming the loosest debris configuration, is of 46,000 m^3, which is consistent with site observations (Romeo et al., 2017).

Static and pseudo-static limit equilibrium (LEM) back-analyses were conducted to estimate mobilized strength and to have preliminary insights into the failure mechanisms. Friction angles along the discontinuities were obtained by upscaling laboratory test on the same geological formation through medium-scale roughness and waviness measured on the UAV model.

Regarding the former objective, the most important result of the LEM analyses is that bridges of intact rock are needed along J1 to explain why the wedge was stable both in static conditions and under seismic actions exerted by the M5.9 October 26th earthquake.

An alternative hypothesis is that the wedge was not completely isolated by joints J1 and J2 but a portion of rock mass at its tip provided additional strength, other than the frictional strength along the two joints.

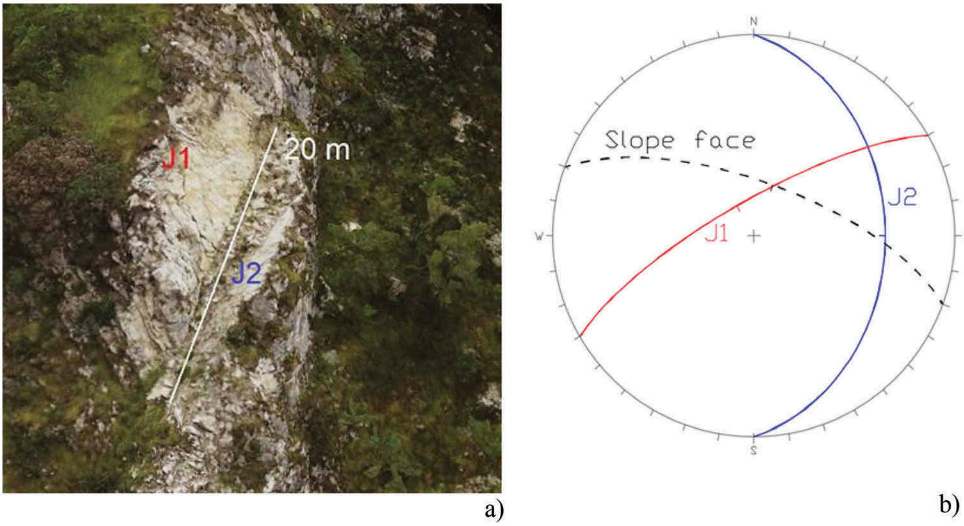

Figure 5. Frontal view from the UAV survey of the Costa Cattiva rock slide (a) and stereo-plot (equal-area projection) of major discontinuities (b). In figure a) the two sliding surfaces are indicated.

Furthermore, failure occurred during the M6.5 October 30th earthquake can be explained by the higher topographic amplification of seismic motion and/or by the progressive degradation under the repeated seismic loading of the strength of the rock bridges or the rock mass at the wedge tip. These two key factors of the instability mechanism are being currently studied with more refined analyses.

4.2 *Costa Cattiva rock slide*

This rock slide detached from the left (southern) flank of the Nera River valley, 2 km east from Visso, fell into the Nera River and threatened the SP 134 highway after a runout of 150 m. It was again a rock wedge slide along two major joints, which involved 300-400 m^3 of bedded limestones (*Maiolica Fm*) with thin layers (about 0.1 m) heavily deformed by folds.

The wedge is delimited by two joints (Figure 5): J1 oriented 75°/330° and J2 oriented 35°/090°. The sliding occurred along their intersection line directed at about 50° and daylighting at low-angle from the slope.

This rock slide presents some similarities with the Nera one: in fact, the sliding planes J1 of the two wedges belong to the same set dipping toward northwest at very high angle (Figure 4b). The wedge was likely a prism, whose outer faces were formed by planes oriented as J1 and J2. Also in this case the bedding planes were not sliding surfaces, as the apparent folding would increase waviness and hence provide additional strength.

4.3 *Piè la Rocca rock slide*

On the northern slope of Mount Patino, about 5 km northeast from Norcia, close to the Piè la Rocca village, the August 24th earthquake triggered several landslides having considerable run-out (up to 400 m) They invaded some forestry roads and hiking trails in the Sibillini Mounts National Park (Figure 6a). The greatest event mobilized about 15,000 m^3 of massive limestone with a wedge-sliding mechanism with a maximum height of about 25 m (Figure 6b).

After an initial planar sliding, the rock wedge, crumbled down the slope towards N knocking down large trees and fragmenting into blocks up to 1,500 m^3 in volume. Some fragmented blocks, about 5-10 m^3 in volume, reached the valley bottom and the hiking trail. The close range photos taken from the drone highlighted many open joints that isolate large blocks standing on the slide scar in precarious stability conditions.

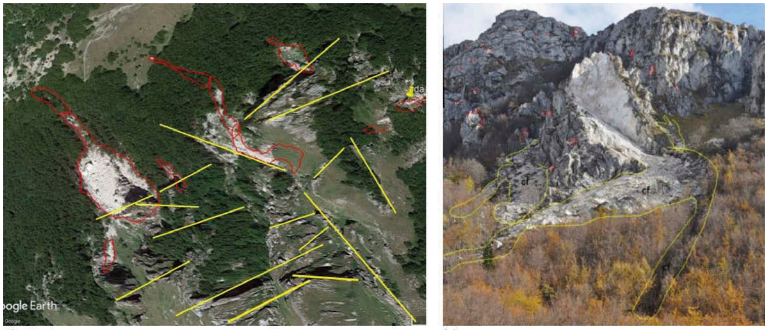

a) b)

Figure 6. Google Earth image of the rock avalanches and rock falls along the northern flank of Mt. Patino, in yellow the main faults (a); frontal picture of Piè la Rocca rock slide showing the avalanche run-out (b).

4.4 *Ponte di Pietra rock slide*

Along the right flank of the Nera River valley, SW of Visso (i.e. downstream from the Nera rock slide), several failures triggered by the seismic events reached the valley bottom without affecting the road. Almost all occurred in the thickly bedded *Calcare Massiccio Fm*. (bedding spacing larger than 1 m).

Among these, the Ponte di Pietra rock slide (Figure 8), mobilized 5,000-7,000 m^3 and generated a rock avalanche with a runout of about 250 m. The slide scar is located 200 m above the valley bottom, on a steep cliff delimiting a gorge that is almost perpendicular to the Nera River (striking 110°).

The geo-structural model (Figure 8) shows the average orientation of the sliding plane that is about 50°/050°. The sliding surface, now covered by debris, is probably formed by a combination of bedding planes, oriented at about 10/020°, and two subvertical joint sets J1 and J2, thus forming the large steps visible along the whole slope. The J2 system, oriented 85°/200°, is parallel to the gorge and is more or less orthogonal to the other, J1 oriented 85°/095°. The 40-m-wide tension crack can be regarded itself as the combination of these two systems. Rock mass folding induces local variations of the estimated bedding attitude.

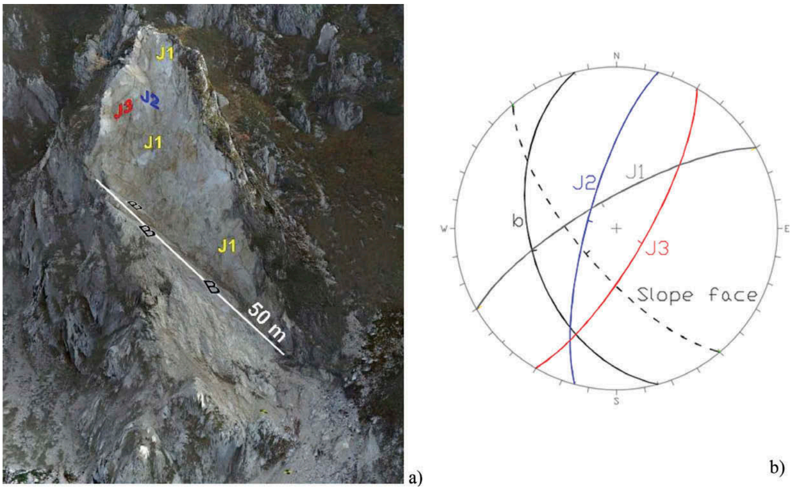

a) b)

Figure 7. UAV front view of the Piè la Rocca rock slide with indication of the discontinuities delimiting the wedge (a); stereoplot (equal-angle projection) of major discontinuities (b).

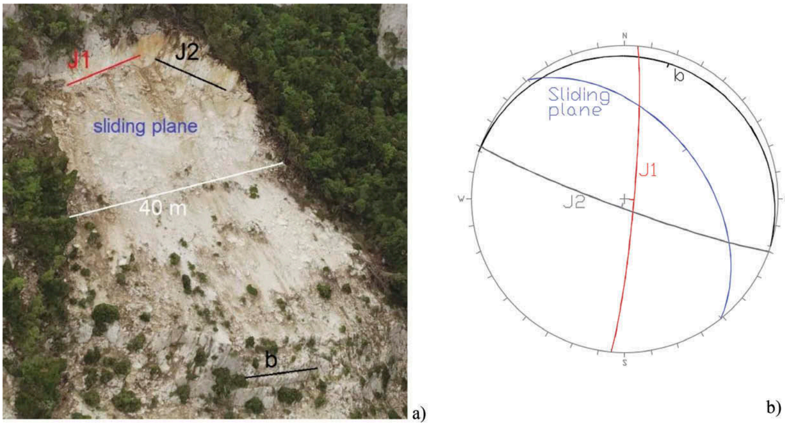

Figure 8. UAV view of the Ponte di Pietra rock slide with indication of the main joint sets (a) and stereoplot (equal-area projection) of joint sets (b).

4.5 *Foce rock slide*

The 2016 earthquakes triggered many rock slides and rock falls on the flank of Mt. Bove and Mt. Vettore, formed by massive limestones (*Calcare Massiccio Fm.*). One of the largest events involved some 30,000 m^3 on the flank of a glacial valley close to the village of Foce, at an elevation of 1700 m a.s.l. The main sliding surface coincided more or less with a persistent bedding joint (Figure 9). The sliding mass was delimited by three major joints: a 75°/120° oriented joint at the back (J1) and two joint J2 and J3 on the lateral sides, oriented 70°/020° and 60°/330° respectively. The landslide debris is formed by large blocks (up to 1,000 m^3) that knocked down high-trunk trees and extended over an area of 30,000 m^2 with a runout exceeding 400 m.

4.6 *Rubbiano rock slide*

This rock slide occurred at the foot of a steep mountain flank in the eastern part of the Mt. Sibillini massif, where the layered limestone of *Maiolica Fm.* overlies the calcareous marls of the *Scaglia Cinerea Fm.* through an apparent thrust plane. The rockslide, located immediately above the tectonic contact, involved about 15,000 m^3 of limestone.

The model obtained by BYU from UAV images shows again that a wedge slid along a major discontinuity (J1 in Figure 10b) oriented about 80°/070°. The back of the wedge is a

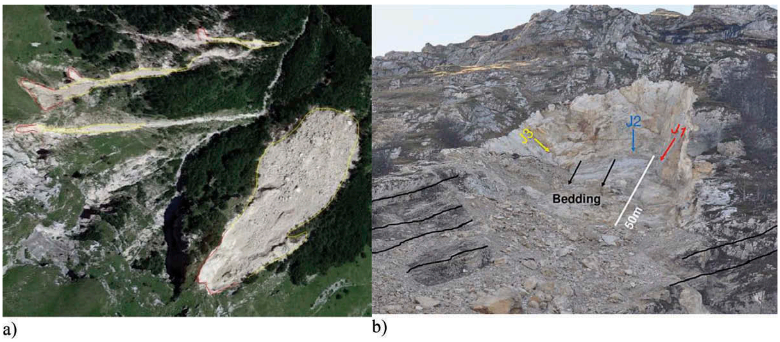

Figure 9. General view (Google Earth image) (a) and front view (b) of the Foce rock slide with indication of the main joint sets.

complex surface with average orientation of 60°/270°, which is composed by a mosaic of joints belonging to different sets, including the J1 set as well and the bedding, here intensely folded. Several joints likely exhibit signs of tensile failure. The cliff is about 70°/115° oriented.

4.7 *Cervaro rock fall*

This rock fall is well representative of a number of events that affected the ledges formed by thick sandstone layers of the *Laga Fm*., on top of mountain slopes of the Laga Mts., in the southernmost part of the earthquake damage area (Abruzzo region). Major events were recorded during the October 30th earthquake. At Cervaro (Figure 11a) the rock mass is

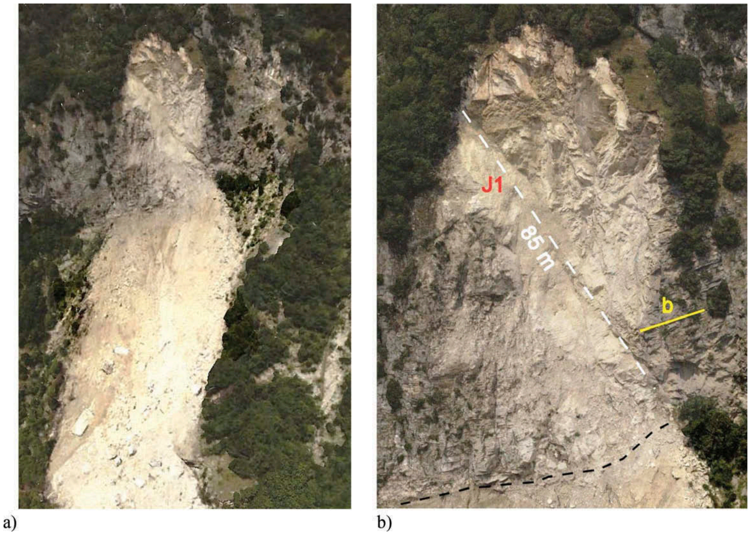

Figure 10. UAV front view of the Rubbiano rock slide (a) and indication of the sliding joint surface, J1, bedding traces, b, and thrust plane trace (dashed line at the picture bottom) (b).

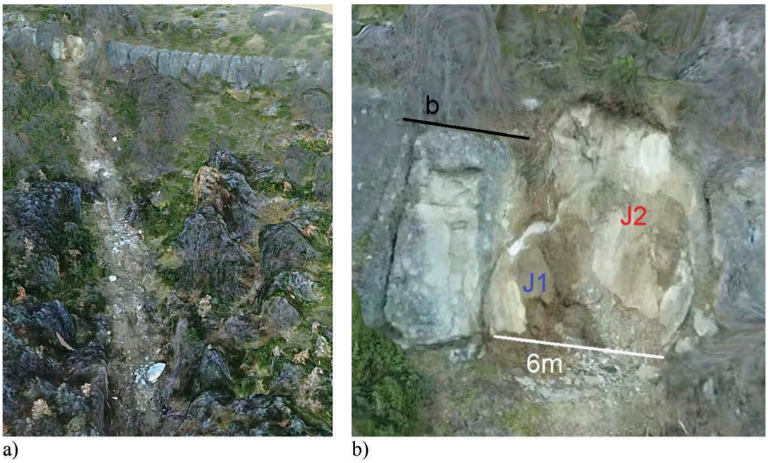

Figure 11. UAV front view of the Cervaro landslide and of the very uppermost part of the runout path (high erosional) (a); detail of the landslide scar the trace of bedding, b, and the main subvertical joint sets (J1 and J2) are indicated (b).

characterized by alternations of sub-horizontal or gently-dipping (some 15°) sandstone layers (up to 8 m thick) and thinner mudstone layers. Field surveys and models based on UAV imagery indicate that vertical fractures normal to the slope face (spaced up to 8-9 m) and tension cracks parallel to the slope crosscut the whole sandstone layer (Figure 11b), thus delimiting blocks tens of cubic meters in volume. The rock fall mobilized about 170 m^3, with a volume of the largest detached block of 55 m^3. The average size of fragmented blocks along the rock fall path (Figure 11a) was 4 m, with a maximum runout distance of 0.5 km (Franke et al., 2018).

5 FAILURE MECHANISMS AND INFLUENCING FACTORS

Earthquake-triggered rock slides occur when the incoming seismic motion at the site, its local dynamic response and the discontinuity orientation and strength combine favourably.

Almost all the rock slides shown in the previous sections occurred during the 30th October 2016 shock. Except for the Piè la Rocca rock slide, epicentral distances are not far enough to have induced noticeable attenuation phenomena. Therefore a single input motion can be assumed for all failures.

Except for the Rubbiano rock slide, the local site response to earthquakes can be considered to be affected only by topographic effects. In fact the stiffness variations within the various slopes do not justify significant impedance contrasts and consequent stratigraphic amplification. Similarly, the reduced stiffness of the shallower loosened portion of the rock mass usually involves a few-meter-thick layer, which is able to amplify only the highest frequencies.

The morphological layout of the investigated area is characterized by deep valleys (200-400 m) with steep flanks, separated by large and flat mountain ridges that can be schematized as high mesas. Therefore the typical profile of a valley flank can be sketched as a steep slope or cliff with a horizontal top plane (step-like slope). The studies available in the literature (Bouckovalas et al., 2005, Ashford et al. 1997) highlighted that along the entire sub-vertical flank the main amplification effect occurs at the fundamental vibration period of the slope, which corresponds to a wave length of about 5H (being H the slope height). In fact recent numerical analyses of an indefinitely high cliff show that if the “oscillating step vertex effect” is not considered, the “vertical-wall” response produces only an attenuation of the motion.

Assuming a shear wave velocity of the involved geological formations in the range 1500-3000 m/s and the typical valley depths, the fundamental frequency varies from 1 to 3 Hz. Further motion amplifications occur: a) at the top segment of the cliff, to an extent as shorter as frequency increases; b) or at local morphological irregularities as buttes, pinnacles or intermediate steps. The phenomenon described at point a) is confirmed by the large number of small rock falls that punctuate the very top of the Nera River Valley flanks. Respect to point b), at least three of the examined cases (Costa Cattiva, Ponte di Pietra and Piè la Rocca) showed that failure occurred at the top of a secondary ridge that spikes along the general trend of the entire valley flank and that could be interested by amplifications for both the fundamental frequency of the slope and higher frequencies.

Rock joints allow the detachment of single wedges but at the same time they constrain motion mode of the wedges. At Nera, Costa Cattiva, Piè la Rocca and Rubbiano rock slides, the wedge is formed by a gentler plane over which the movement developed and a sub-vertical plane that did not provided a relevant shear strength. In seismic conditions, the resulting force applied to the wedge has a horizontal component that favours the detachment from a sub vertical plane with tensile failure of rock bridges and hence an abrupt drop of resistance. Successively, due to the orientation of the joints delimiting the wedge, sliding occurs on a single plane and collapse can be reached earlier, compared to sliding along the joint intersection line, through a fall/toppling mechanism.

At Rubbiano the general mechanism seems to involve a sliding motion on a single plane. Local seismic response due to the limestone-marl stiffness contrast was investigated through a 1D numerical code (Kottke et al., 2008). The analysis was performed through a linear visco-elastic model, using a uniform damping factor D = 1%. The assumed elastic properties of the rocks were based on geophysical borehole measurements in the same geological formations performed within 100 km from the site. The 30th November accelerometer record from the RAN T1212 station (close to Norcia) was used. The response at the gravity centre of the slide is independent from the limestone overburden, but is featured by a sensible shift of the predominant period (at about 1.5 s) respect to the outcrop signal, with a general attenuation of the motion amplitude. This higher period, associated to a longer wavelength, could have increased the instantaneous inertial forces applied to the relatively large volume of the wedge.

In rock slopes carved in layered limestones (*Maiolica Fm.*) sliding was not recognized along bedding joints, even when they were oriented favourably to this kinematics (i.e., Rubbiano), whilst rock slides in massive limestone (with larger bedding joint spacing) often occurred along bedding. This evidence, which requires further investigation, could be explained by considering that thin layers are usually folded at small scale thus providing higher waviness and variable orientation, and hence higher shear strength.

At Cervaro and neighbouring rock fall sites in the *Laga Fm.*, no evidence of major rock falls was noticed during the August 24th and October 26th events, but these earlier events may have cyclically degraded the strength and the stiffness at the top of the mudstone bed and decreased block interlocking. Similarly, there is no clear evidence of rock falls caused by the M6.3 2009 L'Aquila main shock (approximately 29 km to the south), though old blocks along the slope indicate that rock falls occurred in the past. Field observations reveal that sandstone layers have a noticeable hanging due to erosion of the underlying mudstone. The instability mechanism could be a secondary toppling of sandstone columns controlled by weathering and erosion of the underlying mudstone, similar to those described by Evans (1981), with superimposition of stiffness/strength degradation induced by repeated cyclic loading.

Franke et al (2018) point out that despite the larger epicentral distance of October 30th event (Table 2), its PHGV (peak horizontal ground velocity), cumulative absolute velocity and Arias Intensity were much higher than in the preceding shocks. These rock falls therefore appear to be cases in which velocity and cumulative energy had a greater effect on triggering rock slope instabilities than peak horizontal ground accelerations; this is consistent with fatigue failures or other mechanisms with some ductility.

Cyclic strength degradation is another important issue that seems to have played an important role in most of the major landslide events described in the previous sections. Besides the sandstone-mudstone contact on the flysch slopes, the high number of loading cycle applied during the main earthquakes seems to have especially affected the rock bridges along persistent joints of limestone formations, both under shear and in tension. In this respect, static and pseudostatic limit equilibrium back analyses of the Nera rock slide indicate that rock bridges were necessary to assure stability in static conditions and also provided sufficient strength to maintain the wedge stable during the M6.0 October 26th. This strength was overcome during the successive shock.

Probably also other shocks of significant magnitude have influenced this phenomenon. This could be the case of the Piè la Rocca rock slide, which on August 24th was also hit by a M5.4 "aftershock" of the Accumoli earthquake, whose epicentre was located at very small distance from the landslide.

6 CONCLUSIVE REMARKS

The 2016 seismic sequence triggered more than 1500 landslide: about half of them occurred on road cuts and involved small volumes (from less than 1 m^3 to few m^3); the remaining part occurred on natural rock slopes and mobilized volumes ranging from few hundreds to few tens of thousands of m^3. Landslides mostly involved the Mesozoic limestones and the sandstone layers of the *Laga* flysch formation. Few events involved quaternary weak rocks (breccias, conglomerates and travertines).

Analysis of data from UAV imagery and field surveys on larger rock slides and rock falls allowed definition of geometry, volumes and instability mechanism of the landslides. In limestone formations wedge sliding was the prevailing mechanism. In several cases sliding likely occurred along a single joint dipping between 40° and 60°, either bedding or tectonic (small faults), whilst the second joint was a high-dip major joint of tectonic origin roughly parallel to the slope face. Volumes were up to 30,000 m^3 and runout distances frequently reached, and sometime exceeded, 500 m.

Within the sandstone layers of the *Laga Fm.*, landslides are controlled by the mudstone layers underlying the sandstone ledges. Since the mudstone is weathered and deeply eroded, external actions, as seismic acceleration, can trigger falls and topples. Volumes rarely exceed 3000 m^3 but runout reaches up to 500 m.

Local seismic response affects seismic failures especially through the topographic effect, except for the Rubbiano rock slide, where stratigraphic conditions appear not to be neglected though further investigations are required.

Epicentral distances (Table 2) indicates that all landslides fall within a distance from the epicentre ranging between 8 and 17 km, below the upper bound epicentral distance – surface wave magnitude curve by Keefer & Wilson (1989), except for the Cervaro rock fall, which plots exactly on this curve. All data plots well below the curve proposed by Silvestri et al. (2006).

The largest impact of landslides induced by the 2016 seismic sequence was the damage to the transportation infrastructures and the prolonged closure to traffic, which influenced both the emergency activities and the post-earthquake management.

The study is still in progress, but the first quantitative analyses are providing first indication on how the combination of seismic input and local geological, topographic and geomechanical conditions influence susceptibility to failure of rock slopes. The study is also evidencing areas with high residual hazard on which detailed analyses are to be focused in order to mitigate risk in the damage area.

ACKNOWLEDGEMENTS

Thanks are due to Eng. Valerio Sabatini and Eng. Davide D'Alberti for the Piè la Rocca UAV survey. Eng. Valentina Tuccio carried out preliminary seismic response analyses for the Nera River Valley. Eng. Marco Mancina (ANAS, National Highways Dept.) and Eng. Monica di Mattia (Highway Dept. of Teramo Province) provided assistance and data for the Nera River Valley and Cervaro landslides, respectively. The Authority for the Sibillini Mts. National Park is gratefully acknowledged for giving permission of conducting surveys in the park area. The research was partially funded by the Italian Civil Protection Department RELUIS project (2018), PR8-UR18-WP2 UNINA (Principal investigator A. Santo), and by Progetto di Ateneo Sapienza 2017 "Site investigations, monitoring and modelling of earthquake induced rockslides triggered by the 2016 Central Italy seismic sequence" (Resp. G. Lanzo). The work was partially carried out within the activity of GEER Association, which is supported by the National Science Foundation (NSF) through the Geotechnical Engineering Program under Grant No. CMMI-1266418. Any opinions, findings, and conclusions or recommendations expressed in this material are those of the authors and do not necessarily reflect the views of the NSF. The GEER Association is made possible by the vision and support of the NSF Geotechnical Engineering Program Directors: Dr. Richard Fragaszy and the late Dr. Cliff Astill. GEER members also donate their time, talent, and resources to collect time-sensitive field observations of the effects of extreme events. This work was also partially supported by the Center for Unmanned Aircraft Systems (C-UAS), a National Science Foundation Industry/University Cooperative Research Center (I/UCRC) under NSF Award No. CNS-1650547 along with significant contributions from C-UAS industry members. UAV flight permits and access to several landslide areas were obtained thanks to the help of Engg. Paola Pagliara and Paola Bertuccioli of Dipartimento della Protezione Civile.

REFERENCES

Ashford, S.A., Sitar, N., Lysmer, J., Deng, N. 1997, Topographic Effects on the Seismic Response of Steep Slopes. *Bulletin of the Seismological Society of America*, 87, 3, 701-709.

Boncio, P., Lavecchia, G. 2000. A geological model for the Colfiorito earthquakes (September-October 1997, Central Italy). *Journal of Seismology*, 4, 345–356.

Boschi, E., Guidoboni, E., Ferrari, G., Valensise, G., Gasperini, P. 1997. Catalogo dei forti terremoti in Italia dal 461 a. C. al 1990, *Pubbl. ING-SGA ING Rome*, Italy, 951 pp. (in Italian).

Bouckovalas, G.D. & Papadimitriou, A.G. 2005. Numerical evaluation of slope topography effects on seismic ground motion. *Soil Dynamics and Earthquake Engineering*, 25, 547–558.

Evans, R.S. 1981. An analysis of secondary toppling rock failures-the stress redistribution method. *Quarterly Journal of Engineering Geology and Hydrogeology*, 14, 77-86.

Franke, K.W., Lingwall, B.N., Zimmaro, P., Kayen, R.E., Tommasi, P., Chiabrando, F., Santo, A. 2018. Phased reconnaissance approach to documenting landslides following the 2016 Central Italy Earthquakes. *Earthquake Spectra*, 34, 4, 1693-1719.

GEER, 2016. Engineering reconnaissance of the 24 August 2016 central Italy earthquake - version 2 (P. Zimmaro and J. P. Stewart, eds.), Geotechnical Extreme Events Reconnaissance Association Report No. GEER-050B. doi: 10.18118/G61S3Z.

GEER, 2017. Engineering reconnaissance following the October 2016 central Italy earthquakes - version 2 (P. Zimmaro and J. P. Stewart, eds.), Geotechnical Extreme Events Reconnaissance Association Report No. GEER-050D. doi: 10.18118/G6HS39.

Hirschmüller, H. 2008. Stereo Processing by Semi-Global Matching and Mutual Information, *IEEE Transactions on Pattern Analysis and Machine Intelligence*, 30, 328-341.

Hirschmüller, H., 2005. Accurate and Efficient Stereo Processing by Semi-Global Matching and Mutual Information, *in Proceedings, IEEE Conference on Computer Vision and Pattern Recognition, June 2005, San Diego, CA, USA*,2, 807-814.

ISPRA, 2016. Report attività svolta da ISPRA in data 25-26/08/2016, 22 pp (in Italian).

Keefer D.K., R.C. Wilson, 1989. Predicting earthquake-induced landslides with emphasis on arid and semi-arid environments. Publication of the Inland Geological Society, 2, 118-149.

Kottke, A.R., & Rathje, E.M. 2008. Technical manual for Strata. *Report No.: 2008/10*. Pacific Earthquake Engineering Research Center, University of California, Berkeley

Lowe D.G., 2004. Distinctive image features from scale-invariant keypoints, *International Journal of Computer Vision*, 60, 91-110.

Martino, S. Bozzano, F., Caporossi, P., D'Angiò, D., Della Seta, M., Esposito, C., Fantini, A., Fiorucci, M., Giannini, L.M., Iannucci, R., Marmoni, G.M., Mazzanti, P., Missori, C., Moretto, S., Rivellino, S., Romeo, R.W., Sarandrea, P., Schilirò, L., Troiani, F., Varone, C. 2017. Ground Effects triggered by the 24th August 2016, Mw 6.0 Amatrice (Italy) earthquake: Surveys and inventorying to update the CEDIT catalogue. *Geografia Fisica e Dinamica Quaternaria*, 40, 1, 77-95.

Quattrocchi, F., Pik, R., Pizzino, L., Guerra, M., Scarlato, P., Angelone, M., Barbieri, M., Conti, A., Marty, B., Sacchi, E., Zuppi, G.M., Lombardi, S. 2000. Geochemical changes at the Bagni di Triponzo thermal spring during the Umbria-Marche 1997–1998 seismic sequence. *Journal of Seismology*, 4, 567–587.

Romeo, S., Di Matteo, L., Melelli, L., Cencetti, C., Dragoni, W., Fredduzzi, A. 2017. Seismic-induced rockfalls and landslide dam following the October 30, 2016 earthquake Central Italy. *Landslides*, 14, 1457–1465.

Silvestri F., Forte G., Calvello M. (2016). Multi-level approach for zonation of seismic slope stability: experiences and perspectives in Italy. In: Aversa S., Cascini L., Picarelli L., Scavia C. (eds.) Landslides and Engineered Slopes, Experience, Theory and Practice, vol. 1, 101-118, CRC Press, Leiden.